Mars Exploration Rovers Entry, Descent, and Landing Trajectory Analysis

Prasun N. Desai* and Philip C. Knocke**

Abstract

The Mars Exploration Rover mission successfully landed two rovers "Spirit" and "Opportunity" on Mars on January 4th and 25th of 2004, respectively. The trajectory analysis performed to define the entry, descent, and landing (EDL) scenario is described. The entry requirements and constraints are presented, as well as uncertainties used in a Monte Carlo dispersion analysis to statistically assess the robustness of the entry design to off-nominal conditions. In the analysis, six-degree-of-freedom and three-degree-of-freedom trajectory results are compared to assess the entry characteristics of the capsule. Comparison of the pre-entry results to preliminary post-landing reconstruction data shows that all EDL parameters were within the requirements. In addition, the final landing location for both "Spirit" and "Opportunity" were within 15 km from the target.

Introduction

* Senior Aerospace Engineer, Exploration Systems Engineering Branch, NASA Langley Research Center, Hampton, VA.
** Member of Engineering Staff, Jet Propulsion Laboratory, Pasadena, CA.

The Mars Exploration Rover (MER) mission's "Spirit" and "Opportunity" spacecrafts successfully landed on January 4th and 25th of 2004, respectively. The Landers were targeted to the equatorial region of Mars with Spirit landing in Gusev crater (14.59° S, 175.3° E) and Opportunity landing in Meridiani Planum (1.98° S, 5.94° W). Each Lander carried a rover to explore the surface of Mars making in-situ measurements. However, these rovers are larger and more capable than the Mars Pathfinder Sojourner rover, accommodating an increased suite of science instruments and capable of traversing greater distances during surface operations. Reference [1] gives an overview of the MER mission.

Both Landers delivered the rovers to the surface utilizing the same entry, descent, and landing (EDL) scenario that was developed and successfully implemented by Mars Pathfinder (MPF) [2]. The capsules decelerated with the aid of an aeroshell, a supersonic parachute, retrorockets, and air bags for safely landing on the surface (see Fig. 1). Reference [3] gives a description of the EDL system.

An overview of the EDL sequence of events is first presented, followed by the entry trajectory requirements and constraints, along with the uncertainties utilized in the Monte Carlo dispersion analysis. A description of the six-degree-of-freedom (DOF) and three-degree-of-freedom trajectory simulations is then provided and the results compared to assess the entry characteristics. A Monte Carlo dispersion analysis was performed to statistically assess the robustness of the entry design to off-nominal conditions to ensure that all EDL requirements were satisfied. For example,

evaluating the attitude dynamics of the capsule during the entry near peak heating and at parachute deployment, along with the parachute deployment conditions (dynamic pressure and Mach number). This information was necessary for defining requirements for the thermal protection and parachute subsystems. Finally, results from the post-landing reconstruction are presented and compared with the pre-entry predictions.

EDL Overview

The MER EDL sequence is illustrated in Fig 1. Upon Mars arrival, the landers were separated from their respective cruise stages 15 minutes prior to atmospheric entry. Parachute deployment is determined by the on-board flight software based on vehicle deceleration measurements obtained from two Litton LN-200 Inertial Measurement Units (IMU); one mounted in the backshell is used in conjunction with another inside the rover. Prior to launch, parachute deployment was nominally targeted to a dynamic pressure of 700 N/m^2 (occurring at approximately 244 s after entry interface) which corresponds to an altitude of ~9.5 km. The heatshield is jettisoned 20 s after parachute deployment. The lander descent along its bridle is initiated 10 s thereafter. At an altitude of 2.4 km above ground level (AGL), a radar altimeter acquires the ground. The radar altimeter, with its antenna mounted at one of the lower corners of the lander tetrahedron, provides distance measurements to the local surface for use by the on-board flight software to determine the solution time for firing the Rocket Assisted Deceleration (RAD) system (at ~120 m AGL) and the Transverse Impulse Rocket

System (TIRS). Airbag inflation occurs approximately 0.5 s prior to RAD/TIRS firing. The objective of the RAD rockets are to zero the vertical velocity of the lander ~12 m above the ground. The bridle is then cut, and the inflated airbag/lander configuration freefalls to the surface. Sufficient impulse remains in the retrorocket motors to carry the backshell and parachute to a safe distance away from the lander.

The MER landers entered Mars' atmosphere directly from their interplanetary transfer trajectories with inertial entry velocities of 5.63 km/s for "Spirit" and 5.70 km/s for "Opportunity". The nominal inertial entry flight-path angle selected for both MER entries was –11.5 deg. For comparison, the MPF inertial entry flight-path angle was steeper having a value of –14.2 deg. The 3-σ inertial flight-path angle error requirement for MER was ±0.25 deg. The nominal MER entry flight-path angle was chosen to be as shallow as possible to accommodate the entry mass, while still satisfying the requirement of maintaining at least a 1.0 deg margin between the 3-σ shallow and the skip-out entries. (Skip-out was defined as the steepest flight-path angle at which the time derivative of the trajectory radius first goes to zero. This situation occurs at a slightly steeper entry angle than a true flyby trajectory.) For MER, the skip-out boundary occurred at an inertial flight-path angle of –9.6 deg.

Hypersonic deceleration is accomplished utilizing an aeroshell. The MER aeroshell is based on the MPF design with only minor changes to increase inside volume (Fig. 2). The aeroshell consists of a forebody heatshield and an aftbody backshell. The forebody shape is a Viking heritage 70 deg half-angle sphere cone. Prior to entry, the

capsule (spinning at 2 rpm) is separated from the cruise stage. The capsule has no active guidance or control systems, so the spin rate maintains its inertial attitude (targeted nominally for zero angle-of-attack at atmospheric interface) during coast. Throughout the atmospheric entry, the passive capsule relies solely on aerodynamic stability for performing a controlled descent through all aerodynamic flight regimes: free molecular, transitional, hypersonic-continuum, and supersonic. The capsule must possess sufficient aerodynamic stability to minimize any angle-of-attack excursions during the severe heating environment. Additionally, this stability must persist through the supersonic regime to maintain a controlled attitude at parachute deployment. Reference [4] provides a description of the MER capsule aerodynamics.

Trajectory Simulation

Entry Trajectory Requirements and Constraints

The MER atmospheric entry trajectory is designed to fit within an envelope of derived requirements and physical constraints based upon the lander hardware design. As such, for a successful landing, all entry requirements must be satisfied. Table 1 lists all the EDL requirements and their specific bound. A Monte Carlo dispersion analysis is performed to assess the satisfaction of these requirements.

Atmosphere Model

The atmosphere model utilized by MER in the entry trajectory design and analysis was the Kass-Schofield model [5]. This model was developed specifically for the two landing sites in an effort to predict the most accurate atmospheric properties that would be encountered during the actual landing times. This model takes into account variations in diurnal, seasonal, positional, and site topography to produce mean density, temperature, and pressure profiles, and their statistical perturbations. Figure 3 shows examples of 5 perturbed density profiles (as a percentage of the mean) produced by the Kass-Schofield model. Also, depicted are the ±3-σ bounds of the density variation. Similarly, another model was created using Mesoscale simulation techniques to predict winds that would be encountered at the two sites [6].

Entry State and Error Covariance

Initial conditions at entry are estimated from orbit determination performed by the MER Navigation Team. Reference [7] gives an in depth description of the Navigation process during the cruise phase to Mars and the determination of the final arrival conditions prior to entry. The inertial flight-path angle error requirement at entry (radius of 3522.2 km) was ±0.25 deg. The actual navigation accuracy obtained for MER yielded extremely small state errors upon Mars arrival for both landings. The day of arrival 3-σ inertial flight-path angle error obtained for "Spirit" and "Opportunity" were ±0.01 deg and ±0.02 deg, respectively.

Cruise-Stage Separation

Based on the final cruise-stage and capsule mass properties, a statistical multi-body separation analysis was performed to predict separation attitude and attitude rate errors. The 3-σ attitude errors predicted in pitch and yaw were ±1.7 deg and ±2.7 deg, respectively. The 3-σ attitude rate errors predicted in pitch and yaw were ±0.4 deg/s and ±0.4 deg/s, respectively, and a 3-σ roll rate error of ±1.2 deg/s. These variations were used as inputs in the Monte Carlo analysis.

Trajectory Analysis

Two trajectory propagation codes were utilized for MER landing dispersion analyses: the Program to Optimize Simulated Trajectories (POST) program [8], and the Atmospheric-Entry Powered Landing (AEPL) program [9]. Both programs used the same aerodynamics database (see Ref. [4]), which provided drag and other aerodynamic coefficients as a function of Mach number and capsule angle-of-attack. Also common between the two programs were the atmospheric density models [5], mesoscale wind models [6], and the spacecraft parameters. Both programs modeled descent configuration changes (heatshield separation, airbag inflation, etc.) and non-instantaneous parachute deployment and retro-rocket firing.

The POST trajectory analysis was performed modeling "six-degree-of-freedom" (6DOF) dynamics, in which all forces and torques on the spacecraft are included, from atmospheric interface to parachute deployment. During this portion of the entry,

the full set of capsule aerodynamics and mass properties were incorporated into the simulation to accurately model the hypersonic descent. From parachute deployment to landing, "three-degree-of-freedom" (3DOF) analysis was used, in which only the drag force is modeled and is assumed to act opposite the wind-relative velocity vector. The POST trajectory simulation seamlessly transitions from 6DOF to 3DOF dynamics within a single continuous simulation.

The version of the AEPL program used for MER employed 3DOF analyses throughout. Since the MER entries were unguided and ballistic, the 3DOF results from AEPL agreed well with the 6DOF/3DOF POST simulation. AEPL was also used in maneuver design, in conjunction with the navigation cruise trajectory propagation and targeting programs.

Monte Carlo Dispersion Analysis

A Monte Carlo dispersion analysis was utilized to statistically assess the robustness of the entry design to off-nominal conditions to ensure that all EDL requirements and constraints are satisfied (see Table 1). The two simulations were employed for the MER project for independent verification of the results. Table 2 lists all the input variables that were randomly varied in the Monte Carlo dispersion analysis, along with their respective variance and distribution type. The analysis includes uncertainties in the initial state vector, capsule mass properties (mass, center-of-gravity, inertia), initial attitude and attitude rates, hypersonic aerodynamic

coefficients, atmospheric density and winds, parachute drag, and drag of various terminal descent configurations.

For both the simulations, 2000 random cases were run using the final navigation orbit determination solution for the entry state vector, along with its uncertainty (see Ref. 7). Results from the 6DOF/3DOF POST and 3DOF AEPL simulations for the final pre-entry predictions are shown in Table 3 for "Spirit" and Table 4 for "Opportunity". The entry trajectory and attitude conditions are given at critical points during the descent, in terms of the statistical mean and 3-σ range. These results presented were the best apriori estimates of the expected entry conditions and their corresponding range. In general, there is excellent agreement between the two simulations. However, the 6DOF/3DOF POST results often have a larger variation than the 3DOF AEPL results. This outcome is due to the capsule rotational dynamics that are modeled in the 6DOF portion of the 6DOF/3DOF POST simulation in the hypersonic flight regime which alter the capsule drag coefficient due to changes in the total angle-of-attack (α_T) arising from uncertainties in the initial attitude/rates, mass properties, and the complete set of aerodynamics.

The pre-entry results indicate that all the entry requirements and constraints were satisfied and well within the design limits. Note, due to an observed dust storm on Mars just weeks prior to arrival, the targeted parachute deployment dynamic pressure was increased from the 700 N/m^2 to 725 N/m^2 for the "Spirit" entry and to 750 N/m^2 for the "Opportunity" entry to raise the deployment altitude. This modification was

made to hedge against the possibility of encountering a lower density profile than predicted which would reduce the parachute deployment altitude, and thus, the descent timeline from parachute deployment to RAD firing. Figures 4 and 5 show the scatter in the parachute deployment conditions for the two entries demonstrating that they were well within the requirements. The overall 99 percentile size of the landing footprints predicted prior to entry for "Spirit" and "Opportunity" were 73 x 8 km and 71 x 10 km, respectively. Reference 10 gives an in depth description of the landing footprint assessments during the final approach to Mars.

Also listed in Tables 3 and 4 for comparison to the pre-entry predictions are preliminary reconstructed trajectory conditions from the actual "Spirit" and "Opportunity" flight data obtained during their respective landings. Accelerometer and gyro flight data were recorded during both descents and the parameters that can be reconstructed from this data set are listed. As seen, almost all the reconstructed parameters are well within the pre-entry predicted 3-σ variations. However, there are a few parameters that are near or slightly exceed the 3-σ variation bounds (e. g., time of and α_T at parachute deployment).

For both the "Spirit" and "Opportunity" entries, the time of parachute deployment was later than predicted because a lower density atmosphere was experienced. Based on preliminary atmosphere reconstruction estimates, approximately an 8% lower density profile (correlating to roughly a 1-σ low profile) was encountered in the maximum deceleration region during the "Spirit" descent, while approximately a 12%

lower density profile was encountered during the “Opportunity” descent. This greater reduction in the density profile for “Opportunity” (as compared to “Spirit”) is consistent with the observed later time of parachute deployment.

An explanation for the higher attitudes for both the “Spirit” and “Opportunity” entries (especially at parachute deployment) has been proposed after analyzing pictures taken by “Opportunity” of its heatshield on the surface of Mars. Inspection of the “Opportunity” heatshield pictures revealed that portions of the thermal blanket assembly remained, and were still attached to the exterior of the heatsield. This blanket assembly was supposed to burn off very early during the entry, but did not. As a result, the aerodynamics properties of both capsules were significantly affected. Estimates of the aerodynamic torques that could arise from these blanket remnants can reproduce the observed attitude excursions. As such, a reasonable root cause that led to the attitude anomaly has been established. Reference [10] describes in detail the investigation and analyses that were performed in developing this explanation for the attitude anomaly.

The landing locations for both “Spirit” and “Opportunity” were within the pre-entry predicted footprint ellipses. “Spirit” landed 13.4 km downrange from its predicted landing location, while “Opportunity landed 14.9 km downrange from its predicted landing location [11]. These downrange landing locations from their desired targets are consistent with experiencing less dense atmospheres during both entries.

Conclusions

The Mars Exploration Rover (MER) mission successfully landed two rovers on Mars. The entry trajectory design including definition of the appropriate trajectory dispersions were critical in the development of the entry, descent, and landing (EDL) system. Monte Carlo dispersion analyses were employed to statistically assess the robustness of the MER entry design to off-nominal conditions. Pre-entry analyses showed that the MER entry design satisfied all EDL requirements. Comparison of preliminary post-landing reconstruction results indicates that both entries met the EDL requirements and were within the variations defined by the pre-entry Monte Carlo dispersion analyses.

Acknowledgment

A portion of this research was carried out at the Jet Propulsion Laboratory, California Institute of Technology, under a contract with the National Aeronautics and Space Administration. The authors gratefully acknowledge the contributions of the entire MER EDL Systems Team and the MER Navigation Team.

References

[1] Roncoli, R. B., and Ludwinski, J. M., "Mission Design Overview for the Mars Exploration Rover Mission," *AIAA/AAS Astrodynamics Specialist Conference and Exhibit*, AIAA-2002-4823, AIAA, Washington, DC, 2002.

[2] Spencer, D. A., Blanchard, R. C., Braun, R. D., Kallemeyn, P. H., and Thurman, S. W., "Mars Pathfinder Entry, Descent, and Landing Reconstruction," *Journal of Spacecraft and Rockets*, Vol. 36, No. 3, 1999, pp. 357-366.

[3] Steltzner, A., Desai, P. N., Lee, W. J., and Bruno, R., "The Mars Exploration Rovers Entry Descent and Landing and the Use of Aerodynamic Decelerators," *AIAA Aerodynamic Decelerator Systems Technology Conference and Seminar*, AIAA-2003-2125, AIAA, Washington, DC, 2003.

[4] Schoenenberger, M., Cheatwood, F. M., and Desai, P. N., "Static Aerodynamics of the Mars Exploration Rover Entry Capsule," AIAA Paper 2005-0056, January 2005.

[5] Kass, D. M., Schofield, J. T., Michaels, T. I., Rafkin, S. C. R., Richardson, M. I., and Toigo, A. D., "Analysis of Atmospheric Mesoscale Models for Entry, Descent, and Landing," *Journal of Geophysical Research*, Vol. 108, No. E12, 25 Nov. 2003, pp. ROV 31-1 to ROV 31-12.

[6] Golombek, M. P., Grant, J. A., Parker, T. J., Kass, D. M., Crisp, J. A., Squyres, S. W., Haldemann, A. F. C., Adler, M., Lee, W., Bridges, N. T., Arvidson, R. E., Carr, M. H., Kirk, R. L., Knocke, P. C., Roncoli, R. B., Weitz, C. M., Schofield, J. T., Zurek, R. W., Christensen, P. R., Fergason, R. L., Andesron, F. S., and Rice Jr., J. W., "Selection of the Mars Exploration Rover Landing Sites," *Journal of Geophysical Research, Planets*, Vol. 108, No. E12, 10 Dec. 2003, pp. ROV 13-1 to ROV 13-48.

[7] D'Amario, L. A., "Mars Exploration Rovers Navigation Results," *AIAA/AAS Astrodynamics Specialist Conference*, AIAA-2004-4980, AIAA, Washington, DC, 2004.

[8] Brauer, G. L., Cornick, D. E., and Stevenson, R., "Capabilities and Applications of the Program to Optimize Simulated Trajectories (POST)," NASA CR-2770, Feb. 1977.

[9] Klumpp, A. R., Atmospheric-Entry, Powered Landing Simulator V4.10C User's Guide, April 23, 2003 (JPL Internal Document).

[10] Tolson, R. H., Willcockson, W. H., and Desai, P. N., "Anomalistic Disturbance Torques During the Entry Phase of the Mars Exploration Rover Missions – A Telemetry and Mars-Surface Investigation," AAS 06-087, February 2006.

[11] Knocke, P. C., Wawrzyniak, G. G., Kennedy, B. M., Desai, P. N., Parker, T. J., Golombek, M. P., Duxbury, T. C., and Kass, D. M, "Mars Exploration Rovers Landing Dispersion Analysis," *AIAA/AAS Astrodynamics Specialist Conference*, AIAA-2004-5093, AIAA, Washington, DC, 2004.

Table 1: EDL Requirements and Constraints

Requirement	Limit
Inertial entry flight-path angle error, deg	< ±0.25
α_T at atmospheric entry, deg	< 10
Max heat rate, W/cm^2	< 57
Max heat load, J/cm^2	< 3815
α_T at max heat rate, deg	< 10
Max stagnation pressure, kPa	< 25
Max deceleration, Earth g	< 8
α_T at parachute deploy, deg	< 13
Dynamic Pressure at parachute deployment, N/m^2	< 900
Mach number at parachute deployment	< 2.1
Mach number at heatshield separation	< 0.6
Deceleration at lander separation, Earth g	< 0.53
Time from parachute deployment to RAD firing, s	> 57
Velocity at RAD firing, m/s	< 93

Table 2: Monte Carlo Analysis Variables

Variable	3-σ Variation	Distribution
Entry states	Based on covariance (See Ref. 7)	—
Mass, kg	±2.3	Gaussian
Radial center-of-gravity offset, mm	±0.325	Gaussian
Axial center-of-gravity, mm	±15.0	Gaussian
Moments of Inertia (Ixx, Iyy, Izz)	1%, 5%, 5%	Gaussian
Cross products (Ixy, Ixz, Iyz), kg-m^2	±0.001, ±0.002, ±1.1	Gaussian
Entry pitch and yaw attitude, deg	±1.7, ±2.7	Gaussian
Entry pitch and yaw rates, deg/s	±0.4, ±0.4	Gaussian
Entry roll rate, deg/s	±1.2	Gaussian
Hypersonic aerodynamic coefficients	See Ref. 4	Gaussian
Parachute C_D	±12%	Uniform
Backshell+Lander C_D	±5% (3-σ)	Gaussian
Lander C_D (airbag stowed)	±20% (3-σ)	Gaussian
Backshell C_D	±5% (3-σ)	Gaussian
Lander C_D (airbag inflated)	±20% (3-σ)	Gaussian
Atmosphere	Kass-Schofield model (See Ref. 5 and 6)	—

Table 3: "Spirit" Monte Carlo Results

		6DOF/3DOF POST		3DOF AEPL		Reconstructed
Parameter	**Units**	**Mean**	**3-σ Range**	**Mean**	**3-σ Range**	
Hypersonic Flight						
Peak Heating Rate	W/cm^2	39.9	38.1-41.7	45.0[b]	42.9[b]-47.1[b]	
Attitude @ Peak Heat Rate	deg	0.6	0-2.2	–[a]	–[a]	1.8
Peak Acceleration	Earth g	5.9	5.5-6.3	5.9	5.5-6.3	5.6
Peak Stag Pressure	N/m^2	9984	9263-10705	9955	9253-10657	
Total Heat Load	J/cm^2	2770	2669-2870	3247[b]	3136[b]-3358[b]	
Parachute Deployment						
Time from Entry	sec	245.6	237.3-253.8	245.5	237.9-253.1	251
Height	km	8.6	6.1-11.1	8.7	6.3-11.1	7.54
Wind-Relative Velocity	m/s	417.7	389.9-445.6	407.0[c]	377.5[c]-436.5[c]	411
Mach Number		1.78	1.71-1.85	1.78	1.71-1.85	
Dynamic Pressure	N/m^2	724.2	654.5-794.0	725.6	654.8-796.3	730
Planet-Relative FPA	deg	-28.2	-30.0- -26.4	-28.1	-29.9- -26.3	
Attitude	deg	1.1	0-4.9	–[a]	–[a]	7
Heatshield Jettison						
Time from Entry	sec	265.6	257.3-273.8	265.5	257.9-273.1	271
Height	km	6.4	3.9-8.9	6.4	4.0-8.8	
Wind-Relative Velocity	m/s	112.2	94.1-130.3	108.9[c]	88.7[c]-129.1[c]	
Planet-Relative FPA	deg	-49.6	-55.6- -43.6	-49.6	-55.7- -43.5	
Dynamic Pressure	N/m^2	60.8	45.2-76.4	–[a]	–[a]	
Mach number		0.47	0.4-0.54	0.47	0.4-0.53	
Lander Descent Initiation						
Time from Entry	sec	275.6	267.3-283.8	275.5	267.9-283.1	281
Height	km	5.6	3.1-8.1	5.6	3.2-8.1	
Wind-Relative Velocity	m/s	90.6	77.4-103.9	90.5[c]	75.1[c]-105.8[c]	
Planet-Relative FPA	deg	-62.0	-70.4- -53.6	-62.1	-70.7- -53.5	
Dynamic Pressure	N/m^2	41.8	31.8-51.8	–[a]	–[a]	
Sensed Acceleration	Earth g	0.43	0.39-0.46	0.43	0.39-0.46	
RAD Initiation						
Time from Entry	sec	345.8	316.2-375.3	346.7	317.3-376.2	339.4
Time from Chute Deploy	sec	100.2	64.4-136.0	101.3	65.3-137.2	88.4
Height	m	123.1	91.3-154.7	118.4	87.1-149.6	99.4
Wind-Relative Velocity	m/s	73.1	61.6-84.5	73.0[c]	61.8[c]-84.2[c]	69.2
Planet-Relative FPA	deg	-83.9	-89.9- -76.3	-84.1	-89.6- -77.4	
Mach number	0.29	0.24-0.34	0.29	0.24-0.33		
Bridle Cut						
Time from Entry	sec	348.2[d]	319.7[d]-376.3[d]	349.7	320.6-378.7	
Height	m	12.4[d]	4.2[d] -20.1[d]	13.6	11.1-16.1	8.5
Wind-Relative Velocity	m/s	9.8[d]	0.2[d] -25.3[d]	9.3[c]	0.3[c]-20.4[c]	11.8
Landing						
Time from Entry	sec	350.5[d]	321.0[d] -379.5[d]	352.3	322.9-381.5	
Wind-Relative Velocity	m/s	13.9[d]	7.2[d] -25.0[d]	13.9[c]	6.7[c]-21.2[c]	14.0

[a]Computed in 6DOF only, [b]Different calculation method used, [c]Planet-relative velocity listed, [d]Results obtained from 24DOF multi-body POST simulation.

Table 4: "Opportunity" Monte Carlo Results

		6DOF/3DOF POST		3DOF AEPL		Reconstructed
Parameter	**Units**	**Mean**	**3-σ Range**	**Mean**	**3-σ Range**	
Hypersonic Flight						
Peak Heating Rate	W/cm^2	42.2	39.3-45.2	47.9[b]	44.6[b]-51.1[b]	
Attitude @ Peak Heat Rate	deg	0.6	0-2.1	–[a]	–[a]	2.1
Peak Acceleration	Earth g	6.4	5.9-7.0	6.4	5.9-7.0	6.3
Peak Stag Pressure	N/m^2	10835	9868-11803	10812	9863-11760	
Total Heat Load	J/cm^2	2711	2595-2826	3190[b]	3064[b]-3317[b]	
Parachute Deployment						
Time from Entry	sec	242.1	234.5-249.7	242.1	235.2-249.0	250.3
Height	km	8.7	6.4-11.0	8.8	6.6-11.0	7.52
Wind-Relative Velocity	m/s	438.0	411.8-464.2	425.3[c]	395.4[c]-455.2[c]	434
Mach Number		1.86	1.78-1.94	1.86	1.79-1.94	
Dynamic Pressure	N/m^2	747.0	674.7-819.3	749.1	676.3-821.9	764
Planet-Relative FPA	deg	-26.8	-28.4- -25.1	-26.7	-28.3- -25.2	
Attitude	deg	1.0	0-4.4	–[a]	–[a]	8
Heatshield Jettison						
Time from Entry	sec	262.2	254.6-269.8	262.1	255.2-269.0	270.3
Height	km	6.5	4.2-8.8	6.5	4.3-8.8	
Wind-Relative Velocity	m/s	116.9	99.3-134.5	113.1[c]	94.1[c]-132.1[c]	
Planet-Relative FPA	deg	-47.6	-53.0- -42.2	-47.6	-53.3- -42.0	
Dynamic Pressure	N/m^2	63.5	47.1-80.0	–[a]	–[a]	
Mach number	0.49	0.42-0.56	0.49	0.42-0.56		
Lander Descent Initiation						
Time from Entry	sec	272.1	264.6-279.8	272.1	265.2-281.8	280.3
Height	km	5.7	3.3-8.0	5.7	3.5-8.2	
Wind-Relative Velocity	m/s	91.0	81.0-106.9	92.1[c]	78.6[c]-113.9[c]	
Planet-Relative FPA	deg	-60.6	-67.5- -53.8	-60.7	-67.8- -53.6	
Dynamic Pressure	N/m^2	43.6	33.0-54.3	–[a]	–[a]	
Sensed Acceleration	Earth g	0.44	0.40-0.49	0.44	0.40-0.48	
RAD Initiation						
Time from Entry	sec	343.7	315.9-371.5	344.7	317.1-372.2	336.3
Time from Chute Deploy	sec	101.5	68.2-134.8	102.5	69.1-136.0	86
Height	m	123.1	91.3-154.7	118.5	85.4-151.7	127.1
Wind-Relative Velocity	m/s	72.7	61.4-84.1	72.7[c]	61.1[c]-84.4[c]	71.1
Planet-Relative FPA	deg	-86.8	-89.9- -80.9	-86.8	-89.9- -80.7	
Mach number		0.29	0.25-0.33	0.29	0.24-0.33	
Bridle Cut						
Time from Entry	sec	347.9[d]	318.6[d] -377.2[d]	347.6	320.4-374.8	
Height	m	13.1[d]	4.5[d] -21.7[d]	13.4	11.4-15.4	6.9
Wind-Relative Velocity	m/s	9.6[d]	0.7[d] -23.6[d]	7.1[c]	0.6[c]-18.5[c]	9.3
Landing						
Time from Entry	sec	348.6[d]	320.3[d] -376.9[d]	350.1	322.8-383.3	
Wind-Relative Velocity	m/s	13.8[d]	6.9[d] -23.5[d]	12.6[c]	5.7[c]-19.5[c]	

[a]Computed in 6DOF only, [b]Different calculation method used, [c]Planet-relative velocity listed, [d]Results obtained from 24DOF multi-body POST simulation.

NOTE: Figures should not be printed in color, black and white is requested.

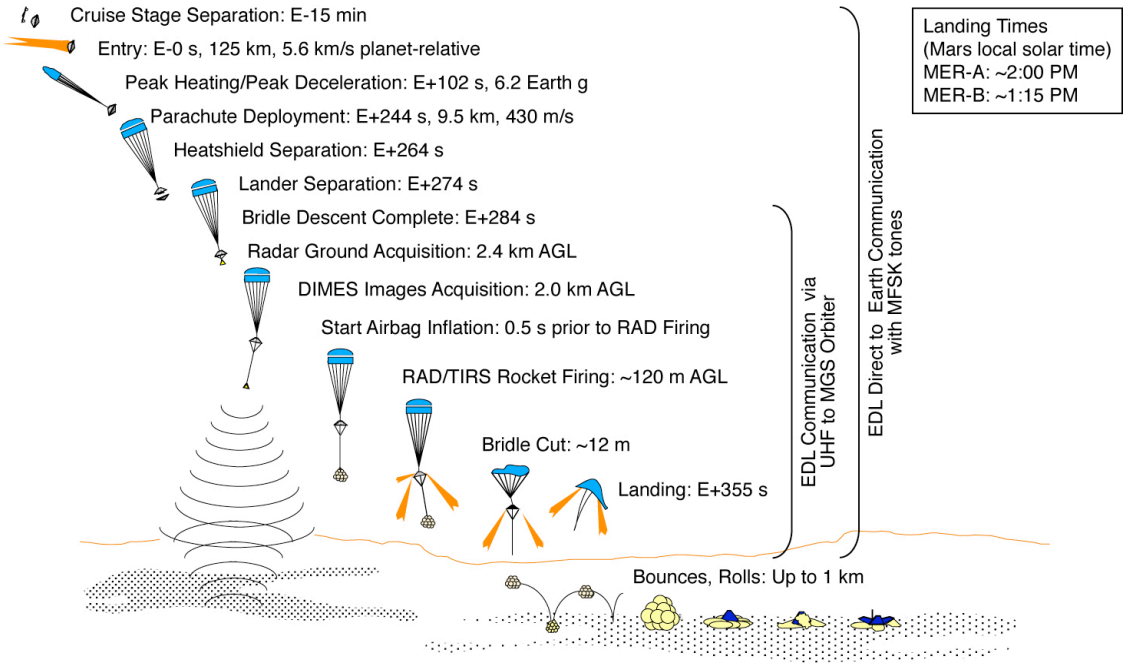

Figure 1. MER Entry, Descent, and Landing Sequence.

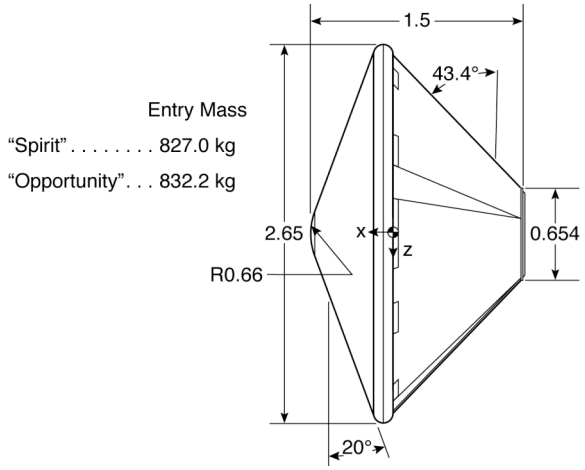

Figure 2. MER Entry Aeroshell Configuration (all dimensions in meters).

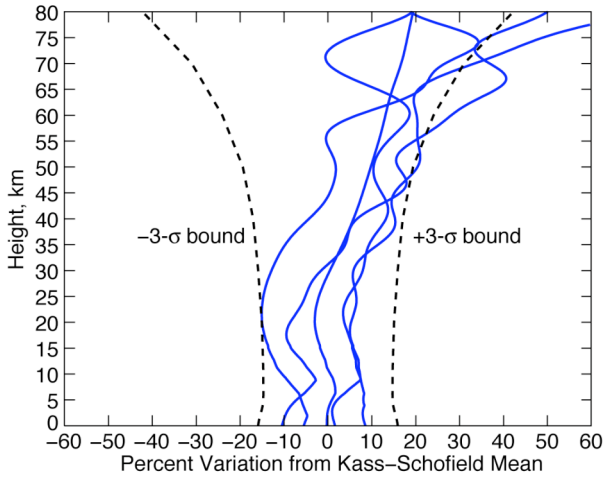

Figure 3. Density Variation from Kass-Schofield Model.

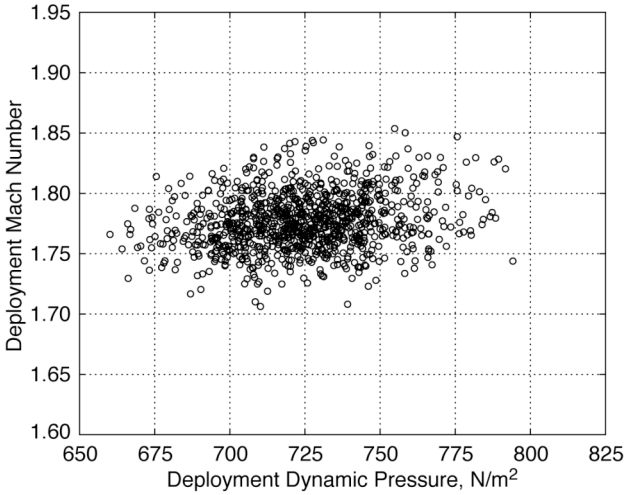

Figure 4. Dispersed Parachute Deployment Conditions from 6DOF Monte Carlo POST Simulation for "Spirit".

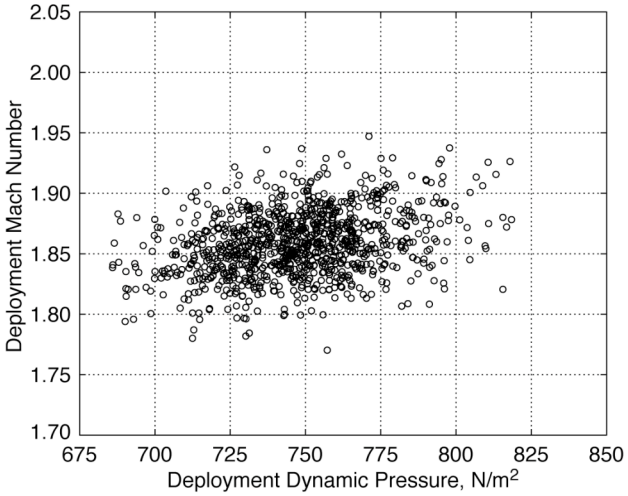

Figure 5. Dispersed Parachute Deployment Conditions from 6DOF Monte Carlo POST Simulation for "Opportunity".